Biosensors and Bioelectronics 33 (2012) 60–68

Contents lists available at SciVerse ScienceDirect

Biosensors and Bioelectronics

journal homepage: www.elsevier.com/locate/bios

Low potential detection of NADH based on Fe_3O_4 nanoparticles/multiwalled carbon nanotubes composite: Fabrication of integrated dehydrogenase-based lactate biosensor

Hazhir Teymourian [c], Abdollah Salimi [a,b,*], Rahman Hallaj [a]

[a] Department of Chemistry, University of Kurdistan, P.O. Box 416, Sanandaj, Iran
[b] Research Center for Nanotechnology, University of Kurdistan, P.O. Box 416, Sanandaj Iran
[c] Department of Chemistry, University of Tarbiat Modares, Tehran, Iran

ARTICLE INFO

Article history:
Received 9 October 2011
Received in revised form
10 December 2011
Accepted 13 December 2011
Available online 26 December 2011

Keywords:
Magnetic nanoparticles
Fe_3O_4
MWCNTs
NADH
Electrocatalytic oxidation
Lactate biosensor

ABSTRACT

Fe_3O_4 magnetic nanoparticles were in situ loaded on the surface of multiwalled carbon nanotubes (MWCNTs) by a simple coprecipitation procedure. The resulting Fe_3O_4/MWCNTs nanocomposite brings new capabilities for electrochemical sensing by combining the advantages of Fe_3O_4 magnetic nanoparticles and MWCNTs. It was found that Fe_3O_4 has redox properties similar to those of frequently used mediators used for electron transfer between NADH and electrode. The cyclic voltammetric results indicated the ability of Fe_3O_4/MWCNTs modified GC electrode to catalyze the oxidation of NADH at a very low potential (0.0 mV vs. Ag/AgCl) and subsequently, a substantial decrease in the overpotential by about 650 mV compared with the bare GC electrode. The catalytic oxidation current allows the stable and selective amperometric detection of NADH at an applied potential of 0.0 mV (Ag/AgCl) with a detection limit of 0.3 μM and linear response up to 300 μM. This modified electrode can be used as an efficient transducer in the design of biosensors based on coupled dehydrogenase enzymes. Lactate dehydrogenase (LDH) and NAD^+ were subsequently immobilized onto the Fe_3O_4/MWCNTs nanocomposite film by covalent bond formation between the amine groups of enzyme or NAD^+ and the carboxylic acid groups of the Fe_3O_4/MWCNT film. Differential pulse voltammetric detection of lactate on Fe_3O_4/MWCNT/LDH/NAD^+ modified GC electrode gives linear responses over the concentration range of 50–500 μM with the detection limit of 5 μM and sensitivity of 7.67 μA mM^{-1}. Furthermore, the applicability of the sensor for the analysis of lactate concentration in human serum samples has been successfully demonstrated.

1. Introduction

The electrochemical oxidation of dihydronicotinamide adenine dinucleotide (NADH) to the corresponding oxidized form (NAD^+) in aqueous solution has received considerable interest, owing to its significance both as a substrate for dehydrogenase enzymes and also to the design of the novel biosensors, because NAD^+/NADH-dependent dehydrogenases constitute the largest group of redox enzymes known today (Bartlett et al., 2002). However, direct electrochemical oxidation of NADH to NAD^+ at the bare electrode surfaces is highly irreversible and takes place at high overpotentials (large activation energy). It is also accompanied by rapid poisoning of the reaction due to the formation of polymeric by-products resulting from unstable and highly reactive one electron oxidation intermediates, leading to surface fouling of electrode (Moiroux and Elving, 1978). In most cases, the high overpotential for NADH electrooxidation has been reduced through the use of mediators. Different electron mediators such as water soluble dye compounds (Maroneze et al., 2008; Santos et al., 2006), catechol and quinone derivatives (Luz et al., 2008; Salimi et al., 2005), phenothiazine derivatives (Gligor et al., 2009a; Santos et al., 2001; Salimi et al., 2010), phenyl azo aniline (Balamurugan and Chen, 2008), adenine derivatives (Alvarez-Gonzalez et al., 2000; Meng et al., 2009) and various redox polymers (Karyakin et al., 2003; Manesh et al., 2008) have been employed to allow for efficient electron transfer, to reduce overpotential, and to prevent surface fouling of electrode. However, although the use of such mediators seems promising, they still cause problems such as leakages from the electrode surface, lack of a long-term stability and toxicity, which have a negative influence on their analytical applications.

Today, with the development of nanoscience and nanotechnology, there have been various trials to employ new nanomaterials in fabricating chemically modified electrodes. Because of their good biocompatibility, strong super paramagnetic behavior, low toxicity, large surface area and easy preparation process, magnetic

* Corresponding author at: Department of Chemistry, University of Kurdistan, P.O. Box 416, Sanandaj, Iran.
E-mail addresses: absalimi@yahoo.com, absalimi@uok.ac.ir (A. Salimi).

0956-5663/$ – see front matter © 2011 Elsevier B.V. All rights reserved.
doi:10.1016/j.bios.2011.12.031

nanoparticles (MNs), especially iron oxide nanoparticles have been widely investigated and applied to immobilize different biomolecules and enzymes (Tanaka and Matsunaga, 2000; Kaushik et al., 2008; Wang et al., 2007; Sulek et al., 2010). The dual analysis of lactate and glucose substrates by the application of relay-NAD^+-cofactor functionalized magnetic particles has also been demonstrated (Katz et al., 2002). On the other hand, carbon nanotubes (CNTs) are considered as an important group of nanostructures with attractive electronic, chemical and mechanical properties (Baughman et al., 2002). The compatibility and electrochemical applications of CNTs to immobilize a variety of species have been reported (Chen et al., 2001; Salimi et al., 2010, 2006, 2007, 2008). Furthermore, it has already been reported that the combination of MNs with CNTs provides hybrid nanocomposites with synergetic effect that leads to the improvement in the electrocatalytic properties of modified electrodes (Miao et al., 2009; Baby and Ramaprabhu, 2010). Thus, MNs/CNTs composite film can be a useful platform for immobilizing biomolecules or enzymes to enhance sensor performances.

Herein, we wish to report on a new electrochemical sensing platform with excellent electrocatalytic activity for NADH electrooxidation based on the Fe_3O_4 magnetic nanoparticles functionalized carbon nanotubes composite (stated as Fe_3O_4/MWCNTs) on glassy carbon electrodes. In contrast to most of previous studies that rely on employment of the mediators or chemical treatment, with our proposed modified electrode, the NADH oxidation would be possible under a very low potential without limitations arising from employment of mediators. Analytical performances of the NADH sensor in terms of the dynamic linear range, sensitivity, selectivity and stability of the electrode were determined.

The successful confinement of dehydrogenase enzyme and NAD^+ cofactor onto the electronic transducers could facilitate the development of integrated electrochemical biosensors and represent a great advance in this research field. Here, using L-lactate dehydrogenase (LDH) as a model enzyme, we have reported a simple and sensitive method for lactate detection based on Fe_3O_4/MWCNTs nanocomposite film coimmobilized with LDH and NAD^+ (stated as Fe_3O_4/MWNTs/LDH/NAD^+).

The rationale for the strategy demonstrated here for simple confinement of LDH and NAD^+ onto the electronic transducer is basically based on the covalent bond formation between amino groups of LDH and NAD^+ and carboxyl groups of Fe_3O_4/MWNTs. First, a uniform layer of Fe_3O_4/MWCNTs was simply formed on the GC surface by casting method. Thereafter, LDH and NAD^+ were immobilized on the Fe_3O_4/MWCNTs modified electrode surface by the amide bond formation between the activated EDC and NHS-treated carboxylic acid groups on the film and the amine groups of the enzyme and NAD^+. Compared with the methods previously employed for surface confinement of NAD^+, the strategy demonstrated here avoids the complex synthetic procedures and thereby offers a simple but effective approach to the general development of integrated dehydrogenase-based biosensors and biofuel cells. Finally, the applicability of the proposed sensor for the analysis of lactate concentration in real samples was demonstrated.

2. Experimental

2.1. Chemicals and reagents

NAD^+ (disodium hydrate), NADH, sodium L-lactate (98%) and L-lactate dehydrogenase from rabbit's muscle (LDH, EC 1.1.1.27 140 Umg^{-1}) were purchased from Sigma. Multiwalled carbon nanotubes (MWCNTs) with purity of 95%, surface specific area of 480 $m^2\,g^{-1}$, diameter of 20–30 nm and 1 μM length were obtained from Nanolab (Brighton, MA). Ferric chloride ($FeCl_3{\cdot}6H_2O$), ferrous chloride ($FeCl_2{\cdot}4H_2O$), *N*-(3-dimethylaminopropyl)-*N*′-ethylcarbodiimide hydrochloride (EDC), *N*-hydroxy succinimide (NHS), NH_3, uric acid (UA), ascorbic acid (AA), glucose (GL), dopamine (DA) and acetaminophen (AP) were prepared from Sigma. Phosphate buffer solutions (PBS, 0.1 M) with different pHs were prepared with sodium dihydrogen phosphate and disodium hydrogen phosphate and used as supporting electrolyte throughout electrochemical studies.

2.2. Apparatus

Transmission electron microscopy (TEM) was performed with a Philips microscope (EM 280, Tokyo, Japan). The magnetic properties were investigated by a home-made alternative gradient force magnetometer (AGFM). Cyclic and differential pulse voltammograms were performed using an AUTOLAB modular electrochemical system (ECO Chemie, Ultrecht, The Netherlands) equipped with a PGSTAT 101 module and driven by NOVA software (ECO Chemie) in conjunction with a conventional three-electrode system and a personal computer for data storage and processing. A modified glassy carbon electrode employed as the working electrode and a platinum wire as the counter electrode. All potentials were referred to an Ag/AgCl/KCl (3 M) electrode. Amperograms were carried out with a Metrohm multi-purpose instrument model 693VA Processor, equipped with a 694VA Stand. A Metrohm drive shaft was used to rotate working electrodes during amperometric detection. Before each experiment, the electrolyte solution was purged with N_2 for at least 10 min to remove dissolved O_2 and kept under N_2 atmosphere during measurements. All electrochemical measurements were performed at room temperature.

2.3. Preparation of Fe_3O_4/MWCNTs nanocomposite modified GC electrode

At first, the carboxylic acid functionalization of MWCNTs was carried out by acid treatment (Kong et al., 2008). Fe_3O_4/MWCNTs nanocomposite was prepared according to a method described previously (Kong et al., 2008) with a slight modification. Briefly, 20 mg of functionalized MWCNTs were dissolved in 20 ml of distilled water in an ultrasonic bath for 20 min. Then 30 mg of $FeCl_3{\cdot}6H_2O$ was added under stirring. After the mixture was stirred vigorously for 30 min under N_2 atmosphere, 40 mg of $FeCl_2{\cdot}4H_2O$ was added and keep stirring under N_2 atmosphere for 30 min. 2 ml of concentrated NH_3 diluted with 10 ml of distilled water was slowly added into the mixture. Adding of NH_3 aqueous solution was completed in 1 h and then the solution was heated to 60 °C and reacted for another 2 h. The whole process must be under N_2 atmosphere. The reaction mixture was then centrifuged, washed with ethanol and distilled water and dried at room temperature. 2 mg Fe_3O_4/MWCNTs nanocomposite was dispersed into 1 ml distilled water by 20 min ultrasonic agitation to give a homogeneous Fe_3O_4/MWCNTs nanocomposite suspension. Fe_3O_4 nanoparticles for AGFM measurement were prepared using the Massart's method (Massart, 1981).

Prior to coating, GC electrode was carefully polished with 3 μM alumina powder on polishing cloth and sonicated successively in ethanol and doubly distilled water in order to remove adsorbed particles. Following that, 4 μL of the Fe_3O_4/MWNTs nanocomposite suspension was cast on the resulting GC electrode surface and allowed to dry at room temperature.

2.4. Preparation of the Fe_3O_4/MWCNT/LDH/NAD^+ modified GC electrode

The LDH and NAD^+ were immobilized onto the Fe_3O_4/MWCNTs surface according to the procedure developed previously (Rahman

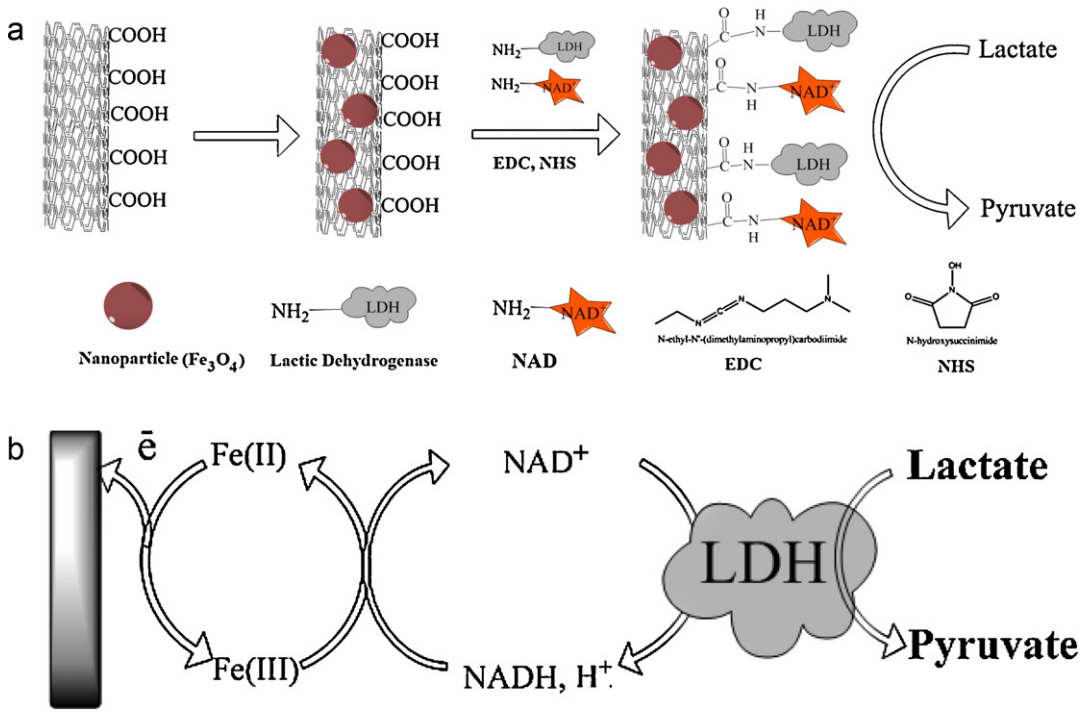

Scheme 1. Schematic representation for (a) the fabrication of Fe_3O_4/MWNTs/LDH/NAD^+ modified GC electrode and (b) the mechanism of bioelectrocatalytic sensing of lactate using this modified electrode.

et al., 2009) with a slight modification (Scheme 1a). First, the Fe_3O_4/MWCNTs modified GC electrode was immersed for 2 h in a 0.1 M PBS (pH 7.0) containing a mixed solution of 10 mM EDC and 10 mM NHS to activate the unbound and free carboxylic groups of Fe_3O_4/MWCNTs nanocomposite layer. Then EDC–NHS treated electrode was washed thoroughly with a 0.1 M PBS (pH 6.8) to remove excess EDC and NHS and was incubated for 3 h in a 0.1 M PBS (pH 7.0) containing 0.5 mg/ml solution of LDH at 4 °C. LDH was immobilized on the Fe_3O_4/MWCNTs modified electrode surface by the amide bond formation between the activated EDC and NHS-treated carboxylic acid groups on the film and the amine groups of the enzyme. After this stable attachment of LDH, NAD^+ was immobilized at remaining unreacted carboxylic acid groups on the Fe_3O_4/MWCNTs layer with the amide bond formation between the activated carboxylic groups of MWCNTs and amine group of NAD^+, by immersing the Fe_3O_4/MWCNTs/LDH modified GC electrode for 2 h in a 0.1 M PBS (pH 6.4) containing 10 mM NAD^+ solution at 4 °C

2.5. Lactate biosensing procedure and blood sample analysis

Scheme 1b shows the lactate biosensing protocol using the Fe_3O_4/MWCNTs/LDH/NAD^+ modified GC electrode. The enzymatic reactions involved in the biosensing system are as follows:

$$\text{Lactate} + NAD^+ \rightarrow \text{Pyruvate} + \text{NADH} + H^+ \quad (1)$$

$$\text{NADH} + Fe_3O_4/\text{MWCNTs} \rightarrow NAD^+ + Fe_3O_4/\text{MWCNTs} \quad (2)$$

In the present study, enzyme LDH catalyzes the oxidation of lactate while the cofactor NAD^+ get reduced to NADH. The NADH generated in the enzymatic reaction is oxidized at the modified electrode. Since the concentrations of NAD^+ and its oxidation products at the surface of electrode are constant, the increase in the electrocatalytic current only depends on the lactate concentration.

Two blood samples taken from two different person's vein were supplied by a clinical diagnostic laboratory. For the lactate determination in plasma using the proposed biosensor, 100 μL of sample was diluted in 2 ml of phosphate buffer solution at pH 7.5. DPVs were conducted to test the practical applicability of the Fe_3O_4/MWCNTs/LDH/NAD^+ modified GC electrode. We performed the lactate determinations in human blood plasma using a standard addition method. In addition, the diluted human plasma samples were spiked by appropriate amounts of lactate and recoveries were calculated. The measurements were carried out in triplicate.

3. Results and discussion

3.1. Characterization of Fe_3O_4/MWCNTs and Fe_3O_4/MWCNTs/LDH/NAD^+ modified GC electrodes

TEM operating at 100 kV was used to reveal the internal structure of the nanocomposite. The TEM samples were prepared by dispersing the nanocomposite in double distilled water with ultrasonic field and then drying a drop of the suspension on a copper grid. The TEM images of MWCNTs and Fe_3O_4/MWCNTs are shown in Fig. 1A. It could be clearly seen that nearly monodispersed Fe_3O_4 (30–40 nm) were attached to MWCNTs. Fine nanotubular morphology without Fe_3O_4 nanoparticles aggregates was obtained. Fig. 1A indicated that a lot of Fe_3O_4 nanoparticles have been adsorbed on the surface of the carbon nanotubes. In TEM image of Fe_3O_4/MWCNTs nanocomposite, the light grey region is carbon nanotubes, indicating that carbon nanotubes were surrounded by Fe_3O_4 nanoparticles.

The magnetic properties of the MWCNTs before and after coated with Fe_3O_4 as well as Fe_3O_4 nanoparticles were examined with AGFM. Fig. 1B shows the room-temperature magnetization of (a) MWCNTs, (b) Fe_3O_4/MWCNTs and (c) Fe_3O_4. It was found that the MWCNTs show no obvious magnetic property, whose saturation magnetization is nearly to zero, while curves (b) and (c) exhibit the same superparamagnetic characteristics. It was found that after coated with Fe_3O_4 nanoparticles, the obtained magnetic carbon nanotubes show superparamagnetic characteristic at room temperature, which are of a higher saturation magnetization as well.

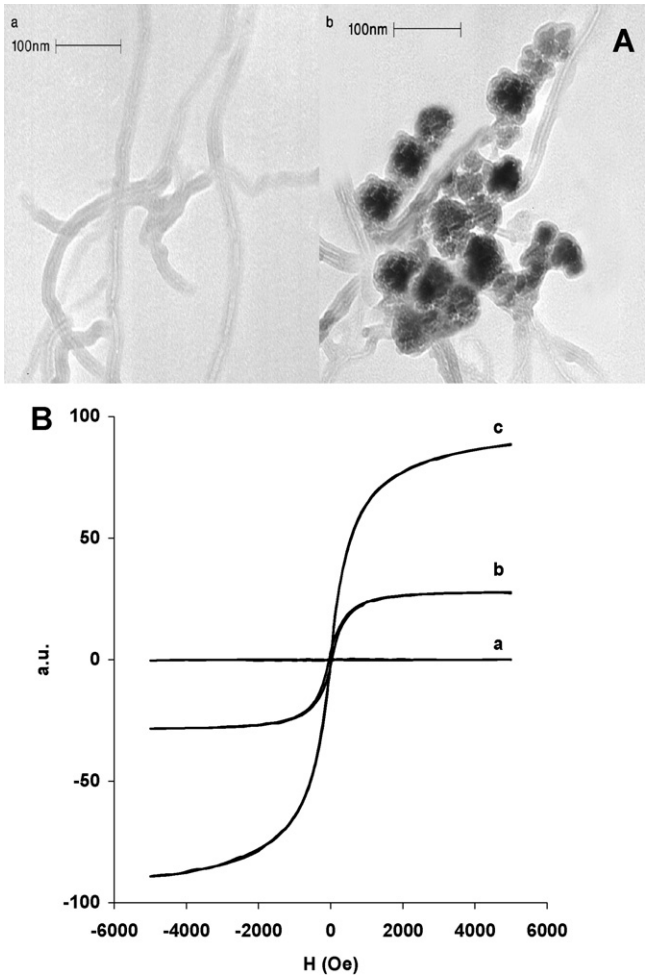

Fig. 1. (A) TEM images of (a) acid-treated MWNTs and (b) Fe_3O_4/MWNTs. (B) Room temperature magnetization of (a) MWNTs, (b) Fe_3O_4/MWNTs and (c) Fe_3O_4.

3.2. Electrochemical behavior of Fe_3O_4/MWCNTs modified GC electrode

After modifying the electrode with Fe_3O_4/MWCNTs, 50 cycles in the potential range from −0.8 up to 0.5 V in 0.1 M PBS at a scan rate of 0.1 V s^{-1} was performed until the electrode provided a stable electrochemical response. The electrochemical behavior of the Fe_3O_4/MWCNTs modified electrode was examined by cyclic voltammetry. The cyclic voltammograms of this modified electrode in a deaerated PBS (pH 7.5) at various potential scan rates were recorded (Fig. S1, Supplementary data). As can be seen, there exist an anodic peak of ca. −0.1 V as well as a cathodic peak of ca. −0.3 V. The separation between cathodic and anodic peak potentials (ΔE_p) is about 120 mV and the ratio of cathodic peak current (i_{pc}) to anodic peak current (i_{pa}) nearly equals to unity. To verify whether this redox behavior was due to the Fe_3O_4 nanoparticles, control experiments were performed without Fe_3O_4 on the bare GC or acid-treated MWCNTs modified GC electrodes and we observed no redox response on bare GC electrode (Fig. S2, Supplementary data, voltammogram "a"). For acid-treated MWCNTs modified GC electrode, the background current was increased due to increasing the surface area of the modified electrode (Fig. S2, Supplementary data, voltammogram "b"). Furthermore, the electrochemical behavior of Fe_3O_4/MWCNTs modified electrode is similar to that of the Fe_3O_4 nanoparticles modified electrode (Zhang et al., 2008) or Fe_3O_4/MWCNTs modified electrode (Kang et al., 2011). In fact, the observed electrochemical behavior for Fe_3O_4/MWCNTs modified electrode may be attributed to the iron phosphate redox system. At first, Fe_3O_4 nanoparticles directly reduced at the electrode surface according to reaction (3):

$$Fe_3O_4(s) + 2e^- + 6H^+(aq) \rightarrow 2Fe^{2+}(aq) + 3H_2O + FeO(s) \quad (3)$$

Then, Fe^{2+} ions produced could combine with phosphate ions in the buffer solution:

$$Fe^{2+}(aq) + HPO_4{}^{2-}(aq) \rightarrow FePO_4(s) + e^- + H^+(aq) \quad (4)$$

Hereafter, the solid $FePO_4$ at the surface of electrode could be responsible for observed redox behavior (McKenzie and Marken, 2001). The plot of anodic and cathodic peak currents vs. scan rate was recorded (inset A of Fig. S1). As can be seen, the peak currents were directly proportional to the scan rate in the whole range studied supported the idea of a surface-confined redox process. Moreover, the plotted ΔE_p vs. log of scan rate (inset B of Fig. S1) shows that at high sweep rates, peak separations begin to increase indicating limitation due to the charge transfer kinetics. Based on the Laviron theory (Laviron, 1979), the heterogeneous electron transfer rate constant (k_s) and charge transfer coefficient (α) can be determined by measuring the variation of peak potential with scan rate. The values of peak potentials were proportional to log(ν) for scan rates higher than 3.0 V s^{-1}. Using the equation $E_p = K - 2.303\,(RT/\alpha nF)\log\nu$, where $K = E^{\circ\prime} - 2.303\,(RT/\alpha nF)\log(RTk_s/nF)$, charge transfer coefficient (α) for proposed redox couple was calculated. Through introducing this value in the following Eq. (3), an apparent surface electron transfer rate constant (k_s) was estimated.

$$\log k_s = \alpha\log(1-\alpha) + (1-\alpha)\log\alpha - \log\left(\frac{RT}{nF\nu}\right) - \frac{\alpha(1-\alpha)nFE}{2.303RT} \quad (5)$$

The values of k_s and α were obtained as 31.09 ($\pm$0.50) s^{-1}, and 0.11, respectively. The large value of heterogeneous electron transfer rate constant indicates high ability of MWCNTs as an electron carrier for promoting electron transfer between Fe_3O_4 nanoparticles and electrode surface. The large number of structural defects on the MWCNTs surface as well as its special nanostructure may act as molecular wires, enhances the direct electron transfer redox systems at its interface. The surface concentration (Γ) of electroactive species on Fe_3O_4/MWNTs modified electrode was estimated by the relationship between I_p and Γ which can be estimated by the Laviron equation (Laviron, 1979):

$$I_p = \frac{n^2F^2\nu A\Gamma}{4RT} \quad (6)$$

According to the Eq. (4), the surface coverage of electroactive species on electrode was about 2.90 ($\pm$0.2) $\times 10^{-10}$ mol cm^{-2}. These results also indicate that high amount of the Fe_3O_4 nanoparticles was loaded on MWCNTs.

Long-term stability is one of the most important properties of sensors, biosensors and bioreactors. The working stability of the Fe_3O_4/MWCNTs modified electrode was verified by monitoring peak currents after successive sweeps of cyclic voltammograms. The peak height remained nearly unchanged after performing 300 cycles in 0.1 M PBS (pH 7.5). Furthermore, the storage stability of the Fe_3O_4/MWCNTs modified electrode was very good as the electrode was found to have reserved (96%) its initial activity for more than 2 weeks when kept in air at room temperature. The high stability of this modified electrode may be attributed to the chemical and mechanical stability of Fe_3O_4/MWCNTs and thus it can be used as a useful platform for immobilizing biomolecules or enzymes to enhance sensor performances.

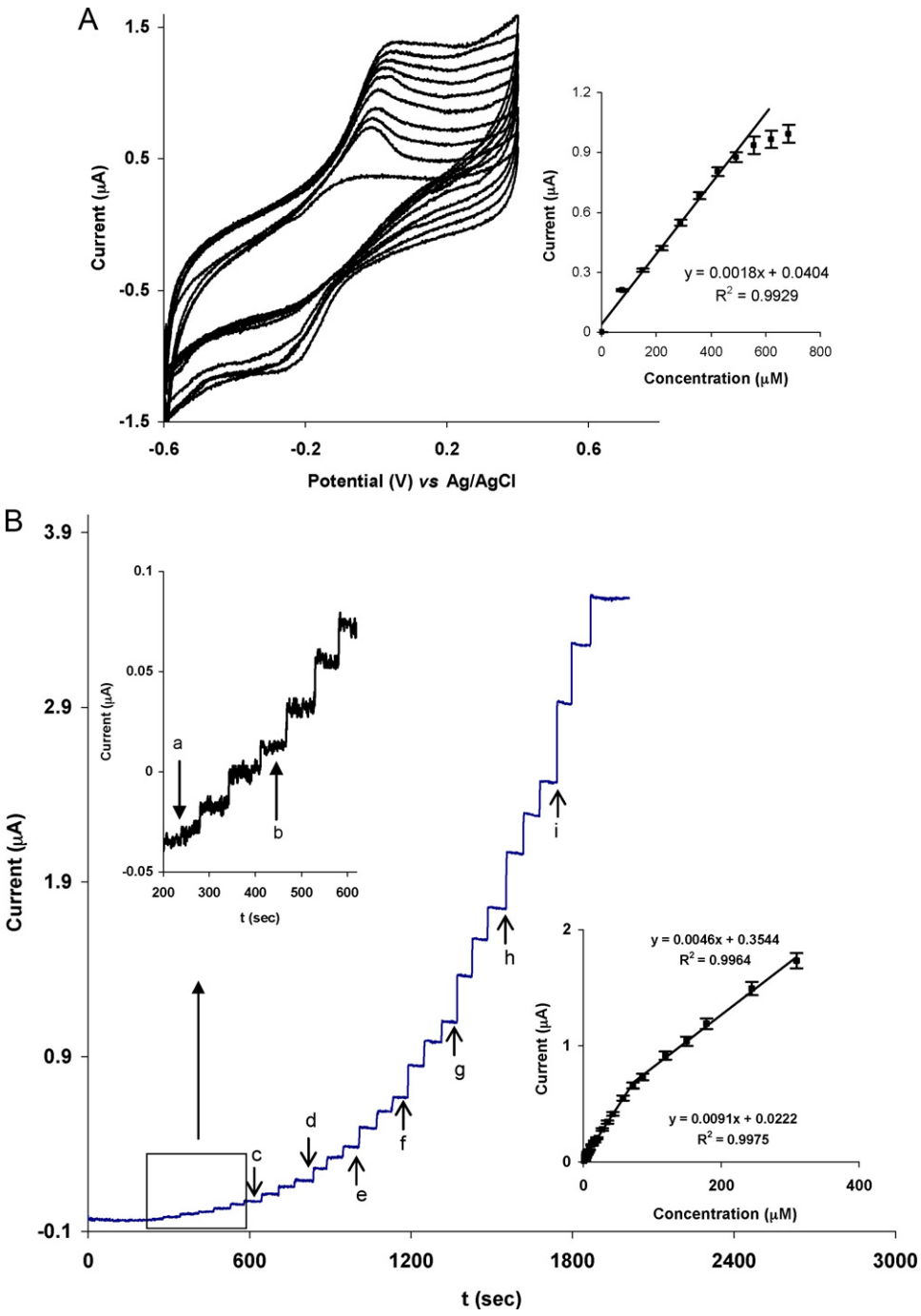

Fig. 2. (A) Cyclic voltammograms of Fe_3O_4/MWNTs modified GC electrode in 0.1 M PBS (pH 7.5) and scan rate 5 mV s^{-1} at different concentrations of NADH (from inner to outer) 0.0, 0.07, 0.15, 0.22, 0.29, 0.36, 0.42, 0.49, 0.55 and 0.62 mM. Inset is the plot of catalytic current vs. NADH concentrations. (B) Chronoamperometric response of Fe_3O_4/MWNTs modified GC electrode in PBS (0.1 M, pH 7.5) on successive addition of different NADH concentrations of (a) 1, (b) 2, (c) 4, (d) 8, (e) 16, (f) 32, (g) 64, (h) 128 and (i) 256 μM (three addition for each concentration) at working potential of 0.0 V vs. Ag/AgCl. Insets are the enlarged view of the defined segment and the Plot of amperometric response vs. NADH concentration (data obtained were the averages of three measurements).

3.3. Electrocatalytic oxidation of NADH on Fe_3O_4/MWCNTs modified GC electrodes

One of the main objectives of this study was to fabricate a modified electrode capable of the electrocatalytic oxidation of NADH. Fe_3O_4 has redox properties similar to those of frequently used mediators used for electron transfer between NADH and electrode. Additionally, due to the electrochemical stability of the corresponding redox couple at Fe_3O_4/MWCNTs nanocomposite modified GC electrode, it can be used as a mediatorless electrochemical system to shuttle electrons between electrode and NADH. In order to examine the electrocatalytic activity of the modified electrode, the cyclic voltammograms were obtained in the absence and presence of different concentrations of NADH at Fe_3O_4/MWCNTs modified GC electrode in PBS (pH 7.5). As shown in Fig. 2A, there is a notable enhancement of anodic peak currents at potentials close to the formal potential of redox couple along with a decrease in the cathodic current with successive additions of NADH. The catalytic currents linearly increased with increasing in NADH concentration up to 500 μM, can be fitted into the equation; I_p

(μA) = 0.0018[NADH] (μM) + 0.0404 μA and R^2 = 0.9929. In order to observe the kinetic characteristics of NADH oxidation by the Fe_3O_4/MWCNTs, cyclic voltammetry of the electrode was investigated with variable scan rates (not shown). The anodic peak current and the peak potential were shifted toward the positive direction with increasing in the scan rate. The excellent linearity shown in the plot of peak current (I_p) vs. the square root of the potential scan rate ($\nu^{1/2}$) confirmed an electrochemical irreversibility of the electrocatalytic reaction and also indicates that this electrocatalytic process is controlled by NADH diffusion from solution to the redox sites of the Fe_3O_4/MWCNTs modified GC electrode. The mechanism of the electrochemical NADH oxidation in the suggested system is as follows:

$$Fe_3O_4/MWNTs + NADH \underset{k_{-1}}{\overset{k_1}{\rightleftarrows}} Fe_3O_4/MWNTs \cdot NADH \xrightarrow{k_2} Fe_3O_4/MWNTs + NAD^+ \quad (7)$$

$$Fe_3O_4/MWNTs{\cdot}NADH \rightarrow Fe_3O_4/MWNTs{\cdot}NADH^{\bullet +} + e^- \quad (8)$$

$$Fe_3O_4/MWNTs{\cdot}NADH^{\bullet +} \rightarrow Fe_3O_4/MWNTs{\cdot}NAD^{\bullet} + H^+ \quad (9)$$

$$Fe_3O_4/MWNTs{\cdot}NAD^{\bullet} \rightarrow Fe_3O_4/MWNTs{\cdot}NAD^+ + e^- \quad (10)$$

Where NADH diffuses and adsorbs on the electrode surface and then it is electrochemically oxidized by an ECE mechanism (Moiroux and Elving, 1980; Kim et al., 2010). According to the ECE mechanism, the first step of NADH electrochemical oxidation is an irreversible heterogeneous electron transfer. In this step, one electron is lost and a cation radical $NADH^{\bullet +}$ is produced in (8). The neutral radical $NAD^{\bullet}$ was produced through a first-order deprotonation reaction of $NADH^{\bullet +}$ in (9). A continual reaction for electron transfer from $NAD^{\bullet}$ occurred through a second heterogeneous electron transfer in (10). In this system, Fe_3O_4 plays the role of an electrocatalyst for NADH oxidation while MWCNTs works as an electron carrier.

Fig. 2B presents the amperometric response of the Fe_3O_4/MWCNTs modified GC electrode at +0.0 V to the successive additions of NADH in 0.1 M PBS (pH 7.5). Immediately after the addition of NADH, the anodic current increased and reached a steady state within 5 s. The sensor response displayed two linear concentration ranges; one from 1.0 to 70 μM with a correlation coefficient of 0.9975 and sensitivity of 0.070 $\mu A\,\mu M^{-1}\,cm^{-2}$ and another one from 70 to 300 μM with a correlation coefficient of 0.9964 and sensitivity of 0.035 $\mu A\,\mu M^{-1}\,cm^{-2}$. The limit of detection (LOD) of this sensing system, which is the minimum concentration at which the ratio of signal to noise is not less than 3, is 300 nM (S/N = 3). The kinetic parameters of this reaction can be estimated by plotting the NADH concentration vs. the current difference (inset of Fig. 2B). This plot showed the kinetics of a heterogeneous second-order reaction type, hence, the affinity of NADH for the electrode ($k_{-1} + k_2/k_1$ in (7)) can be estimated by a Michaelis–Menten constant (K_M) calculation; the value was 95 μM, deduced from a Lineweaver–Burk plot. The obtained K_M is significantly lower compared to other reported values of 3.04 mM (Kim et al., 2010), 0.54 mM (Kim and Yoo, 2009), 2.12×10^{-4} M (Santos Alvarez et al., 2005) and 0.8 mM (Gligor et al., 2009b).

The effect of pH of contact solution on the current responses of Fe_3O_4/MWCNTs modified GC electrode was studied over the pH range of 6.5–9.5 in order to see how it affects the activity of the sensing layer (Fig. S3, Supplementary data). The amperometric currents obtained at different pH values for 20 μM NADH in 0.1 M PBS showed that the amperometric response at pH 7.5 was somewhat higher than other pHs and therefore PBS at pH 7.5 was used throughout experiments.

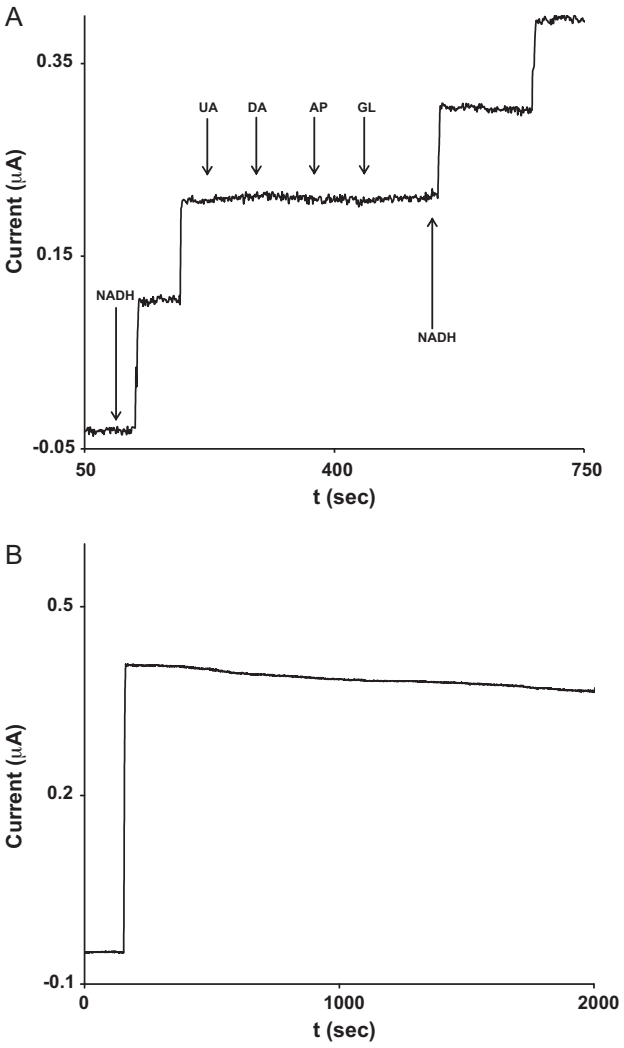

Fig. 3. (A) Amperometric response of the Fe_3O_4/MWNTs modified GC electrode in 0.1 M PBS solution (pH 7.5) containing 20 μM NADH, spiked with UA (0.1 mM), DA (0.1 mM), AP (0.1 mM) and GL (0.1 mM). (B) Amperometric response recorded over a continuous 4000 s of 50 μM NADH in 0.1 M PBS (pH 7.5) at Fe_3O_4/MWNTs modified GC electrode. Working potential is 0.0 V vs. Ag/AgCl.

The common problem in the electrochemical determination of NADH is the interference from redox active species, such as AA, UA, DA, GL and AP. The effects of these common interfering species on the amperometric response of electrode were evaluated (Fig. 3A). The addition of 0.1 mM of each of UA, DA, GL and AP compounds almost did not cause any interference on the current response to a solution containing 20 μM NADH. However, when 0.1 mM of AA was added, its response would be comparable with the NADH response. It seems that Fe_3O_4/MWCNTs also show an electrocatalytic activity toward AA and this compound exhibits a positive interference for NADH detection. Nevertheless, the concentration of AA in real samples rarely is so high that leads to significant interference. Thus, the use of a low operating potential greatly reduced the interference; and thus, a selective response to NADH was obtained without the use of perm-selective membrane. This obviously is another advantage of the proposed sensor.

Another attractive feature of our proposed electrode was its highly stable amperometric response to NADH. Fig. 3B presents the amperometric response of Fe_3O_4/MWCNTs modified GC electrode to 50 μM NADH recorded over a continuous period of 2000 s. As can be seen, the response of the Fe_3O_4/MWCNTs modified GC electrode remained nearly stable with only 10% current diminutions

Table 1A
Response characteristics of different NADH sensors[a].

Electrode	Electrode modified material	$E_{appl.}$ (mV vs. Ag/AgCl)	LOD (μM)	Linear range (μM)	Sensitivity	Ref.
Mediated systems						
GC	Nafion/CNTs/DHB	−50	0.1	0.5–400	11.1 nA μM^{-1}	Raj and Chakraborty (2006)
$SiO_2/SnO_2/Sb_2O_5$	MB	−50	0.15	80–900	8.1 μA mM^{-1}	Canevari et al. (2011)
SiO_2/TiO_2/graphite	MB	−120	8.0	18–7290	0.58 μA mM^{-1}	Maroneze et al. (2008)
GC	PBCB/SWCNTs	0.0	1.0	3–104	9.89 nA μM^{-1}	Yang and Liu (2009)
GC	Th/CNTs/nafion	−100	1.0	2–400	4.70 mA M^{-1}	Huang et al. (2007)
EPPG	TCBQ/MWCNTs	150	0.15	0.5–2160	0.32 μA μM^{-1}	Luz et al. (2008)
Mediator-free systems						
GC	Ploy 3-MT/CNTs	300	0.17	0.5–20	3 μA μM^{-1}	Agui et al. (2007)
GC	Boron doped CNTs	300	0.05	Up to1405	2.25 μA mM^{-1}	Deng et al. (2008)
GC	PP/MWCNTs	600	10.0	20–800	40.37 nA μM^{-1} cm^{-2}	Yuan et al. (2011)
GC	Graphene	500	20.0	50–1400	12.6 μA mM^{-1}	Guo et al. (2011)
GC	IL/MWCNT/chitosan	300	0.06	0.2–26	0.0844 μA μM^{-1}	Wang et al. (2007)
Fe_2O_3/CB	–	0	10.0	10–1000	2.54 μA mM^{-1}	Kim et al. (2010)
GC	Fe_3O_4/MWCNTs	0	0.3	1–70	0.070 μA μM^{-1} cm^{-2}	This study
				70–300	0.035 μA μM^{-1} cm^{-2}	This study

[a] DHB, 5,5′-dihydroxy-4,4′-bitryptamine; s; MB, meldola's blue; PBCB, poly (brilliant cresyl blue); Th, thionine; EPPG, edge plane pyrolytic graphite; TCBQ, 2,3,5,6-tetrachloro-1,4-benzoquinone; poly 3-MT, poly-(3-methylthiophene); PP, diphenylalanine peptide; IL, ionic liquid; CB, carbon black.

after 2000 s. Thus, this electrode can be used as an excellent electrocatalytic material for sensitive and stable amperometric detection of NADH. Moreover, the reproducibility of the Fe_3O_4/MWCNTs modified GC electrode for NADH detection was examined. The chronoamperometric signals produced by a series of five successive measurements of 10 and 100 μM NADH yielded good reproducibilities with the relative standard deviations of 4.5 and 4.7%, respectively.

Table 1A lists the response characteristics of the proposed NADH sensor compared to the some other NADH sensors reported in the literature. The results presented in Table 1A obviously show that the different characteristics of the proposed NADH sensor based on Fe_3O_4/MWCNTs nanocomposite modified GC electrode are better in some cases or comparable with the other sensors reported so far.

3.4. 3.4. Lactate biosensing on Fe_3O_4/MWCNTs/LDH/NAD^+ modified GC electrode

Using LDH as the model biorecognition element, we demonstrated the use of the Fe_3O_4/MWCNTs/LDH/NAD^+ nanobiocomposite as an electronic transducer for the development of integrated electrochemical biosensor for lactate. Fig. 4A shows the cyclic voltammograms of Fe_3O_4/MWCNTs/LDH/NAD^+ modified GC electrode in 0.1 M PBS (pH 7.5) at different concentrations of lactate. As indicated, the anodic peak current increased with increasing lactate concentration. The catalytic currents linearly increased with increasing lactate concentration in the range up to 2.3 mM with sensitivity of 1.065 μA mM^{-1}.

Due to the higher sensitivity of pulse techniques, differential pulse voltammograms of Fe_3O_4/MWCNTs/LDH/NAD^+ modified GC electrode for different concentrations of lactate were recorded (Fig. 4B). This observation clearly supports that the increasing in peak observed at −0.1 V is due to the oxidation of enzymatically produced NADH during lactate oxidation. The calibration plot drawn between the response current and the concentration of lactate (0.05–0.5 mM) is found to be linear (R^2 = 0.9929) with sensitivity of 7.67 μA mM^{-1}, and the detection limit was calculated as 5 μM (based on S/N = 3). These results clearly indicate that detection limit, linear concentration range and sensitivity of the proposed biosensor are comparable or in some cases, better than reported values for different lactate biosensors described in literature; 7.5 μM, 0.1–10 mM and 3.46 μA mM^{-1} cm^{-2} for meldola blue/MWCNT modified carbon paste electrode (Pereira et al., 2007), 1 μM, 5–90 μM and 0.0106 μA μM^{-1} for conducting polymer/MWCNT modified gold electrode (Rahman et al., 2009), 3.8 μM, 10–70 μM and 0.326 A M^{-1} cm^{-2} for ferrocene-methanol/laponite/chitosan hydrogel modified electrode (Zanini et al., 2011), 0.55 mM, 0.55–10 mM and 4.2 nA mM^{-1} for meldola blue/reinecke salt modified screen printed electrode (Piano et al., 2010), 0.76 μM, 5–120 μA and 0.0083 A M^{-1} cm^{-2} for MWCNT/chitosan modified electrode (Tsai et al., 2007). These data further confirm the efficiency of Fe_3O_4/MWCNTs nanocomposite both as a mediatorless electrocatalyzing material and also as an excellent platform for immobilization enzyme and cofactor.

In order to estimate the applicability of the methodology, the proposed lactate biosensor was tested by applying it to the measurement of lactate concentration in two human plasma samples by DPV technique. The standard addition method was performed to demonstrate the possibility of lactate detection in human blood samples and the obtained results were compared with a standard spectrophotometric method (Table 1B). It could be seen that there is a good agreement between results obtained by two methods and also between the spiked and found values for the detection of lactate. A good average recovery of 101.9% was calculated for six measurements. Therefore, the Fe_3O_4/MWCNTs/LDH/NAD^+ modified GC electrode might be a promising system for detecting lactate in real samples.

Table 1B
Determination of lactate in plasma samples.

Sample	Ref. method (mM)	Biosensor (mM)	Added (mM)	Expected conc. (mM)	Obtained conc. (mM)	R.S.D. (%)	Recovery (%)
1	0.228	0.233	–	–	–	2.1	102.19
			0.1	0.328	0.332	4.23	101.21
			0.2	0.428	0.425	3.67	99.30
2	0.204	0.209	–	–	–	3.81	102.45
			0.1	0.304	0.313	3.37	102.96
			0.2	0.404	0.402	5.10	99.50

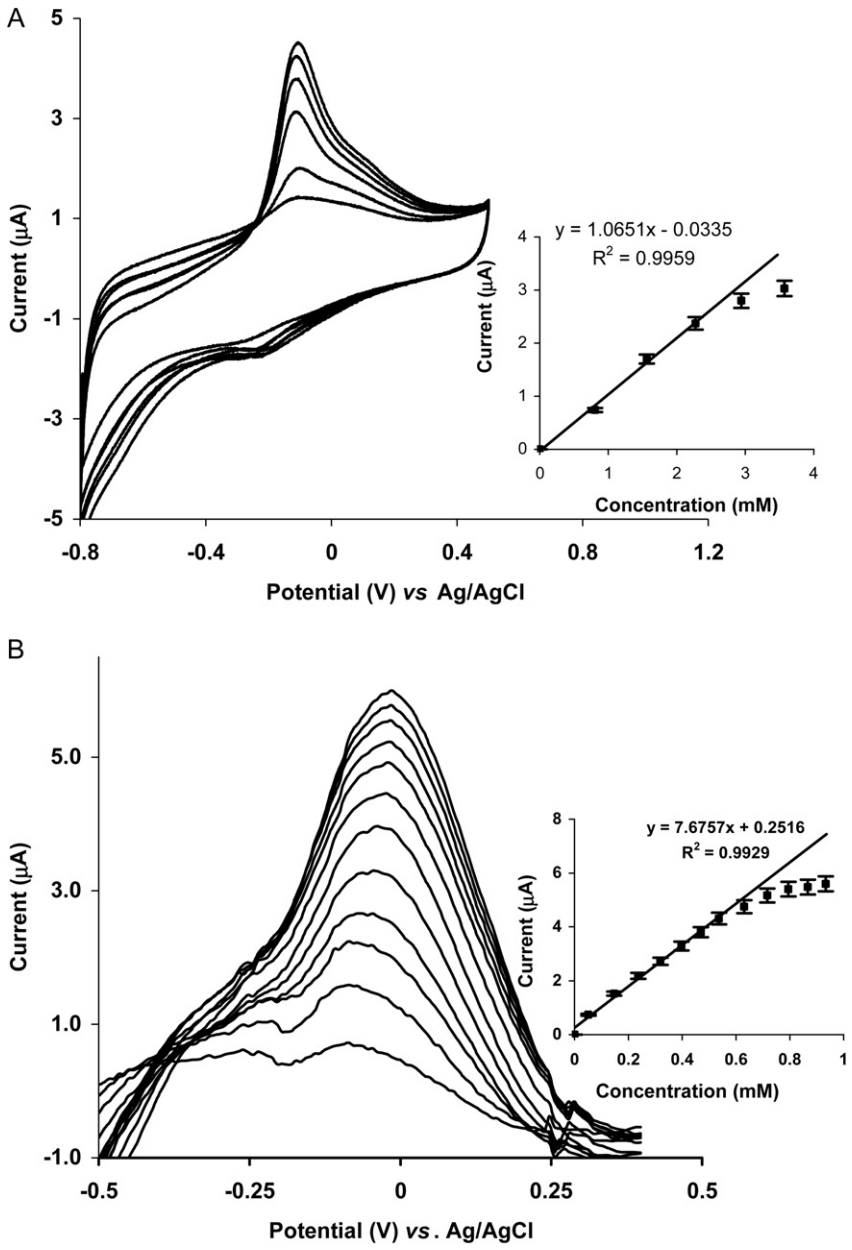

Fig. 4. (A) Cyclic voltammograms of Fe_3O_4/MWNTs/LDH/NAD^+ modified GC electrode in 0.1 M PBS (pH 7.5) and scan rate of 10 mV s^{-1} at different concentrations of lactate, (from inner to outer) 0.0, 0.8, 1.6, 2.3, 2.9 and 3.6 mM. Inset is the obtained calibration plot for lactate. (B) Differential pulse voltammograms of Fe_3O_4/MWNTs/LDH/NAD^+ modified GC electrode in 0.1 M PBS (pH 7.5) at different lactate concentrations, (from inner to outer) 0.0, 0.05, 0.1, 0.18, 0.25, 0.28, 0.3, 0.35, 0.45, 0.52, 0.66, 0.78 and 1.0 mM. Inset is the plot of peak currents vs. lactate concentration (data obtained were the averages of three measurements).

4. Conclusion

In summary, using a simple coprecipitation method, MWCNTs were decorated with iron oxide magnetic nanoparticles. After modifying the electrode with this nanocomposite, a pair of well-defined peaks with low background and high peak current and formal potential at ca. −0.2 V appeared that could be ascribed to the iron phosphate redox system. TEM and AGFM techniques were used to characterize the Fe_3O_4/MWCNTs nanocomposite and the electrochemical behavior of modified electrode has been investigated by cyclic voltammetry. It was found that NADH can be oxidized by the Fe_3O_4/MWCNTs modified GC electrode with significantly lowering the overpotential in neutral pH media. Iron oxide nanoparticles are responsible for observed catalytic activity and MWCNTs has the role of electron carrier. Chronoamperometric detection exhibits a linear dependency on the NADH concentration, with a detection limit of 0.3 μM at linear range up to 300 μM. The high sensitivity and reproducibility, wide linear range and the minimal surface fouling combined with the attractive low potential of the NADH oxidation make this nanocomposite electrode an extremely promising candidate to serve as the electrochemical substrate for fabricating biosensors that incorporate dehydrogenase enzymes. Using LDH as a model enzyme, we have reported a simple and sensitive method for lactate detection based on Fe_3O_4/MWCNTs nanocomposite film coimmobilized with LDH and NAD^+. The sensitivity and detection limit of the biosensor are 5 μM and 7.67 μA mM^{-1} at concentration range up to 0.5 mM. Finally, the developed biosensor was applied to detect lactate concentration in human serum samples and satisfactory results were obtained. Thus, this study suggests that the Fe_3O_4/MWCNTs electrode is a promising candidate for

biosensor design. By employing electrochemical oxidation coupled with the enzyme reaction systems, various kinds of chemicals can be detected.

Acknowledgements

This research was supported by the Iranian Nanotechnology Initiative and the Research Offices of the University of Kurditan and University of Tarbiat Modares.

Appendix A. Supplementary data

Supplementary data associated with this article can be found, in the online version, at doi:10.1016/j.bios.2011.12.031.

References

Agui, L., Pena-Farfal, C., Yanez-sedeno, P., Pingarron, J.M., 2007. Electrochim. Acta 52, 7946–7952.
Alvarez-Gonzalez, M.I., Saidman, S.B., Castanon, M.J.L., Ordieres, A.J.M., Blanco, P.T., 2000. Anal. Chem. 72, 520–527.
Baby, T.T., Ramaprabhu, S., 2010. Talanta 80, 2016–2022.
Balamurugan, A., Chen, S.M., 2008. Sens. Actuators B 129, 850–858.
Bartlett, P.N., Simon, E., Toh, C.S., 2002. Bioelectrochemistry 56, 117–122.
Baughman, R.H., Zakhidov, A.A., de Heer, W.A., 2002. Science 297, 787–792.
Canevari, T.C., Vinhas, R.C.G., Landers, R., Gushikem, Y., 2011. Biosens. Bioelectron. 26, 2402–2406.
Chen, R.J., Zhang, Y., Wang, D., Dai, H., 2001. J. Am. Chem. Soc. 123, 3838–3839.
Deng, C., Chen, J., Chen, X., Xiao, C., Nie, Z., Yao, S., 2008. Electrochem. Commun. 10, 907–909.
Gligor, D., Balaj, F., Maicaneanu, A., Gropeanu, R., Grosu, I., Muresan, L., Popescu, I.C., 2009a. Mater. Chem. Phys. 113, 283–289.
Gligor, D., Dilgin, Y., Popescu, I.C., Gorton, L., 2009b. Electrochim. Acta 54, 3124–3128.
Guo, K., Qian, K., Zhang, S., Kong, J., Yu, C., Liu, B., 2011. Talanta 85, 1174–1179.
Huang, M., Jiang, H., Zhai, J., Liu, B., Dong, S., 2007. Talanta 74, 132–139.
Kang, S.Z., Chen, H., Mu, J., 2011. Solid State Sci. 13, 142–145.
Karyakin, A.A., Ivanova, Y.N., Karyakina, E.E., 2003. Electrochem. Commun. 5, 677–680.
Katz, E., Sheeney-Haj-Ichia, L., Buckmann, A.F., Willner, I., 2002. Angew. Chem. Int. Ed. 41, 1343–1346.
Kaushik, A., Solanki, P.R., Ansari, A.A., Ahmad, S., Malhotra, B.D., 2008. Electrochem. Commun. 10, 1364–1368.
Kim, Y.H., Yoo, Y.J., 2009. Enzyme Microb. Technol. 44, 129–134.
Kim, Y.H., Kim, T., Ryu, J.H., Yoo, Y.J., 2010. Biosens. Bioelectron. 25, 1160–1165.
Kong, L., Lu, X., Zhang, W., 2008. J. Solid State Chem. 181, 628–636.
Laviron, E., 1979. J. Electroanal. Chem. 101, 19–28.
Luz, R.C.S., Damos, F.S., Tanaka, A.A., Kubota, Y., Gushikem, L.T., 2008. Electrochim. Acta 53, 4706–4714.
Manesh, K.M., Santhos, P., Gopalan, A., Lee, K.P., 2008. Talanta 75, 1307–1314.
Maroneze, C.M., Arenas, L.T., Luz, R.C.S., Benvenutti, E.V., Landers, R., Gushikem, Y., 2008. Electrochim. Acta 53, 4167–4175.
Massart, R., 1981. IEEE Trans. Magn. 17, 1247–1248.
McKenzie, K.J., Marken, F., 2001. Pure Appl. Chem. 73, 1885–1894.
Meng, L., Wu, P., Chen, G., Cai, C., Sun, Y., Yuan, Z., 2009. Biosens. Bioelectron. 24, 1751–1756.
Miao, Y., Wang, H., Shao, Y., Tang, Z., Wang, J., Lin, Y., 2009. Sens. Actuators B: Chem. 138, 182–188.
Moiroux, J., Elving, P.J., 1978. Anal. Chem. 50, 1056–1062.
Moiroux, J., Elving, P.J., 1980. J. Am. Chem. Soc. 102 (21), 6533–6538.
Pereira, A.C., Aguiar, M.R., Kisner, A., Macedo, D.V., Kubota, L.T., 2007. Sens. Actuators B: Chem. 124, 269–276.
Piano, M., Serban, S., Pittson, R., Drago, G.A., Hart, J.P., 2010. Talanta 82, 34–37.
Rahman, M.M., Shiddiky, M.J.A., Rahman, M.D.A., Shim, Y.D., 2009. Anal. Biochem. 384, 159–165.
Raj, C.R., Chakraborty, S., 2006. Biosens. Bioelectron. 22, 700–706.
Salimi, A., Hallaj, R., Ghadermazi, M., 2005. Talanta 65, 888–894.
Salimi, A., Mamkhezri, H., Mohebbi, S., 2006. Electrochem. Commun. 8, 688–696.
Salimi, A., Mamkhezri, H., Hallaj, R., Zandi, S., 2007. Electrochim. Acta 52, 6097–6105.
Salimi, A., Miranzadeh, L., Hallaj, R., 2008. Talanta 75, 147–156.
Salimi, A., Lasgary, S., Noorbakhsh, A., 2010. Electroanalysis 22, 1707–1716.
Santos Alvarez, D.N., Lobo Castanon, M.J., Miranda Ordieres, A.J., Tunon Blanco, P., Abruna, H.D., 2005. Anal. Chem. 77, 2624–2631.
Santos, A.S., Ortea, M., Paneda, A.M., Castanon, M.J.L., Ordieres, A.J.M., Blanco, P.T., 2001. J. Electroanal. Chem. 502, 109–117.
Santos, A.S., Pereira, A.C., Duran, N., Kubota, L.T., 2006. Electrochim. Acta 52, 215–220.
Sulek, F., Drofenik, M., Habulin, M., Knez, Z., 2010. J. Magn. Magn. Mater. 322, 179–185.
Tanaka, T., Matsunaga, T., 2000. Anal. Chem. 72, 3518–3522.
Tsai, Y.C., Chen, S.Y., Liaw, H.W., 2007. Sens. Actuators B: Chem. 125, 474–481.
Wang, Q., Tang, H., Xie, Q., Tan, L., Zhang, Y., Li, B., Yao, S., 2007. Electrochim. Acta 52, 6630–6637.
Yang, D.W., Liu, H.H., 2009. Biosens. Bioelectron. 25, 733–738.
Yuan, J., Chen, J., Wu, X., Fang, K., Niu, L., 2011. J. Electroanal. Chem. 656, 120–124.
Zanini, V.P., Mishima, B.L., Solis, V., 2011. Sens. Actuators B: Chem. 155, 75–80.
Zhang, L., Zhai, Y., Gao, N., Wen, D., Dong, S., 2008. Electrochem. Commun. 10, 1524–1526.